HHS Public Access

Author manuscript

Angew Chem Int Ed Engl. Author manuscript; available in PMC 2017 January 11.

Published in final edited form as:

Angew Chem Int Ed Engl. 2016 January 11; 55(2): 539–544. doi:10.1002/anie.201508060.

Activation of electron-deficient quinones through hydrogen-bond-donor-coupled electron transfer

Amanda K. Turek, **David J. Hardee**, **Andrew M. Ullman**, **Daniel G. Nocera***, and **Eric N. Jacobsen***

Department of Chemistry and Chemical Biology, Harvard University, Cambridge, MA 02138 (USA)

Abstract

Quinones are important organic oxidants in a variety of synthetic and biological contexts, and they are susceptible to activation toward electron transfer through hydrogen bonding. While this effect of hydrogen bond donors (HBDs) has been observed for Lewis basic, weakly oxidizing quinones, comparable activation is not readily achieved when more reactive and synthetically useful electron-deficient quinones are used. We have successfully employed HBD-coupled electron transfer as a strategy to activate electron-deficient quinones. A systematic investigation of HBDs has led to the discovery that certain dicationic HBDs have an exceptionally large effect on the rate and thermodynamics of electron transfer. We further demonstrate that these HBDs can be used as catalysts in a quinone-mediated model synthetic transformation.

Graphical abstract

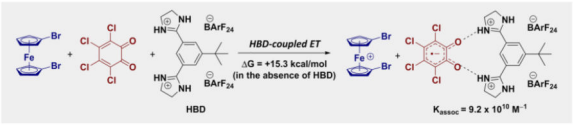

Electron Transfer Made Easier. Electron transfer to electron-deficient quinones is facilitated through use of dicationic hydrogen-bond donors (HBDs). Large thermodynamic barriers to electron transfer are surmounted through strong association between the HBD and the reduced quinone. The use of an HBD is also shown to induce rate accelerations of up to 12 orders of magnitude in electron transfer events (~12 orders of magnitude).

Keywords

quinones; hydrogen bonding; electron transfer; oxidation; catalysis

Hydrogen bonding influences the rates and product distributions of many organic reactions of interest through direct stabilization of transition structures and reactive intermediates.[1,2] In a largely different context, H-bonding is also known to have a significant effect on the

* dnocera@fas.harvard.edu, jacobsen@chemistry.harvard.edu.

Supporting information for this article is available on the WWW under http://www.angewandte.org

thermodynamics and kinetics of electron transfer,[3–13] especially in biological systems. Quinones are especially important cofactors that play critical roles in electron transfer (ET) pathways, including that of photosystem II.[14,15] In this system, a quinone serves as the terminal electron acceptor in a chain of ET events. Hydrogen bonds formed within the quinone binding site play a critical role in stabilizing the semiquinone radical anion after ET,[16] governing a conformational shift[17] that is proposed to constitute the rate-determining step for the first ET to the quinone.[18]

With the knowledge that the behavior of quinones is strongly influenced by H-bonding interactions, we became interested in employing small-molecule hydrogen-bond donors (HBDs) to activate quinone oxidants in a synthetically interesting context. The effect of H-bonding on the redox chemistry of quinones has been investigated in synthetic model systems using a variety of HBDs, including simple alcohols,[3,4] ammonium salts,[5] amino acids,[6] amides,[7,8] and neutral dual HBDs such as ureas[9,10] and thioureas.[11] While these important studies revealed that HBDs can indeed couple with ET to enhance the reactivity of quinone oxidants, this effect was only observed with weakly oxidizing quinones that are good Lewis bases. In contrast, the HBDs used in these studies had little discernible effect on the ET to electron-deficient quinones (Figure 1), which bear electron-withdrawing substituents that increase their oxidizing ability but diminish their Lewis basicity and binding ability.

From a thermodynamic standpoint, HBD-coupled ET using quinone oxidants (equation (1)) can be parsed into two elementary steps: ET between the quinone (**Q**) and an electron donor (**D**, equation (2)), and binding of the reduced quinone to a HBD (equation (3)). While the actual transformation does not need to proceed by this mechanism (e.g., binding of the HBD to **Q** may precede ET), dissection of the overall process in this manner is instructive in defining the challenge that is presented to achieving favorable ET reactions ($\Delta G_{net} < 0$) using HBDs.

$$\mathrm{HBD} + \mathbf{Q} + \mathbf{D} \rightleftharpoons \mathrm{HBD}{\bullet}\mathbf{Q}^{\bullet-} + \mathbf{D}^{\bullet+} \; (\Delta G_{net}) \tag{1}$$

$$\mathbf{Q} + \mathbf{D} \rightleftharpoons \mathbf{Q}^{\bullet-} + \mathbf{D}^{\bullet+} \; (\Delta G_{ET}) \tag{2}$$

$$\mathrm{HBD} + \mathbf{Q}^{\bullet-} \rightleftharpoons \mathrm{HBD}{\bullet}\mathbf{Q}^{\bullet-} \; (\Delta G_{assoc}) \qquad \Delta G_{net} = \Delta G_{ET} + \Delta G_{assoc} \tag{3}$$

The activating effect of a HBD on the overall reaction can be understood in terms of equation (3), which describes binding of the HBD to the reduced quinone ($\mathbf{Q}^{\bullet-}$). That interaction must offset the thermodynamic penalty of the ET (given a $\Delta G_{ET} > 0$), which depends on the substrate **D** and the intrinsic oxidizing ability of the quinone. Oxidation of organic functional groups of interest (e.g. alkenes, aromatic rings) by electron-rich quinones is so unfavorable that an unattainably high binding energy (ΔG_{assoc}) would be necessary to enable the overall reaction by HBDs. ET in synthetically interesting contexts with electron-deficient quinones is less unfavorable.[19] However, as noted above, these quinones and their reduced counterparts are inherently weak H-bond acceptors. As such, the success of the proposed HBD-coupled ET strategy relies on finding the appropriate balance of HBD strength and quinone reactivity.

Herein, we report a systematic evaluation of several small-molecule hydrogen bond donors, with the goal of activating electron-deficient quinones (Figure 2). *o*-Chloranil (**Q**) was selected as the oxidant, as it is an electron-deficient quinone that nonetheless lacks the intrinsic reactivity necessary to oxidize many organic substrates of synthetic interest. Our examination of the influence of H-bonding on the single-electron transfer chemistry of *o*-chloranil has led to the discovery that dicationic *bis*-amidinium salts can exert remarkable influence on the thermodynamics and kinetics of ET. By taking advantage of this effect, we demonstrate that these HBDs can also catalyze a model oxidative transformation that is mediated by *o*-chloranil.

Electrochemical quantification of binding

In aprotic media, quinones undergo two sequential single-electron transfers, proceeding through the semiquinone radical anion $\mathbf{Q}^{\bullet-}$.[20] Protic and H-bonding molecules influence the mechanism by which ET proceeds. This study is concerned primarily with the effect of HBDs on the first ET step. To quantify the ability of a HBD to modulate the thermodynamics of ET, the association of HBDs with $\mathbf{Q}^{\bullet-}$ must be quantified —or, in other terms, how strongly the HBD favors the reduced state over the oxidized, neutral state.

The mechanistic tools used to quantify HBD-coupled ET are borrowed from the study of proton-coupled ET.[21] Equation (4), which is related to the Nernst equation, describes HBD-coupled ET (Scheme 1a). The apparent potential of a quinone involved in HBD-coupled ET will undergo a shift ($\Delta E_{1/2}$) that is dependent on the HBD concentration and the association constants for the binding of the quinone and semiquinone (K_Q and $K_{Q^{\bullet-}}$, respectively) to the HBD.

$$\Delta E_{1/2} = 0.059V log \frac{1+K_{Q^{\bullet-}}[HBD]}{1+K_Q[HBD]} \quad (4)$$

This relationship between $\Delta E_{1/2}$ and the association constants shows that, as long as $K'_{Q^{\bullet-}} > K'_Q$, increasing concentration of the HBD results in a more positive $\Delta E_{1/2}$, effectively creating a more potent oxidant by favoring the reduced state through binding. As the square scheme in Scheme 1a illustrates, $K'_{Q^{\bullet-}}$ specifically describes this stabilizing interaction. The

equilibrium constants that govern this shift in the potential can be elucidated electrochemically through cyclic voltammetry and provide a quantitative measure of the stabilization provided by the HBD to $\mathbf{Q}^{\bullet-}$.

Results and Discussion

1. Electrochemical studies

Our investigations were carried out with a range of HBDs, including representative dual HBDs **1**–**3**, with the aim of understanding how H-bonding interactions affect ΔG_{assoc} (equation (3)) when electron-deficient quinones are used. Electrochemical titrations of **Q** were performed with each HBD, using cyclic voltammetry to record the $\Delta E_{1/2}$ as a function of HBD concentration (Figures 3a–c). Each of the HBDs studied has a significant, measurable effect on the apparent potential that corresponds to the first ET.[22] Additionally, the reversibility of the CVs recorded in all titration experiments indicate that the effect on $E_{1/2}$ is the result of H-bonding to $\mathbf{Q}^{\bullet-}$ and not protonation, which would manifest as irreversibility in the CV traces.

To elucidate the equilibrium constants that describe binding of $\mathbf{Q}^{\bullet-}$ to **1–3**, the full set of electrochemical data for these titrations was subjected to simulations.[23] This analysis reveals that the experimental data are best described by a mechanism in which two HBD molecules are involved in stabilization of $\mathbf{Q}^{\bullet-}$. This mechanistic interpretation provides a good fit to the experimental data with respect to the overall $\Delta E_{1/2}$, and also reproduces the distinct features of the cyclic voltammogram at low [HBD] (for example, as in Figure 3a, scan (b) and corresponding simulation (f)).[24]

An HBD-coupled ET to **Q** that involves two binding events requires the use of an expanded square scheme to outline all mechanistic possibilities (Scheme 1b), wherein $K_{1Q^{\bullet-}}K_{2Q^{\bullet-}}$ provides a quantitative description of the stabilization provided to $\mathbf{Q}^{\bullet-}$ through binding, and a measure of the oxidizing strength of **Q** in the presence of a given HBD.

The electrochemical simulations allow us to distinguish between the pathways for HBD-coupled ET outlined in Fig. 1d and elucidate the binding constants associated with each individual step. The simulations for **1–3** reveal that these HBDs each promote a mechanism in which binding of the neutral quinone (K_{1Q}) precedes ET (E_2), and a second binding event follows ($K_{2Q^{\bullet-}}$).[25] Simulation of this mechanism explicitly determines values for these equilibrium constants, from which $K_{1Q^{\bullet-}}$ can be calculated. Independent determination of K_{1Q} values using spectroscopic methods was consistent with those obtained from the simulations (Supporting Information, Figures S1–S4).

The values for $K_{1Q^{\bullet-}}K_{2Q^{\bullet-}}$ were determined in this manner for HBDs **1**–**3** and are summarized in Table 1. All three HBDs afford similar results with respect to mechanism and stoichiometry (Figures 3b and 3c). Diphenylguanidinium **2** offers the greatest degree of stabilization to $\mathbf{Q}^{\bullet-}$ and urea **3** offers the weakest, with a difference of three orders of magnitude between them. A comparison of these values provides insight into the ways in which the nature of the HBD can influence its interaction with $\mathbf{Q}^{\bullet-}$. The enhanced binding of **2** relative to **1** can be ascribed to a difference in acidity[26] Such an effect implicates hydrogen

bonding interactions in the modulation of ΔG_{assoc} and increased favorability of ET to **2**. On the other hand, neutral **3** and cationic **1** have similar pK_a values,[27] yet $K_{1Q^{\bullet-}}$ $K_{2Q^{\bullet-}}$ for **3** is smaller by an order of magnitude, demonstrating the importance of electrostatic effects in HBD-coupled ET. Combined with the requirement of 2:1 stoichiometry between the HBD and $\mathbf{Q}^{\bullet-}$, this result has important implications for the HBD-coupled ET strategy, as the data from the titration with **2** clearly indicate that the most substantial stabilization of $\mathbf{Q}^{\bullet-}$ is achieved in a complex that involves two cationic HBDs. We conclude that both H-bonding and electrostatic effects play a crucial role in HBD- coupled ET.

The observation that HBDs **1**–**3** all bind $\mathbf{Q}^{\bullet-}$ in 2:1 complexes, with the charge of the HBD playing a critical role, prompted us to examine *bis*-amidinium salt **4**,[28] which involves a covalent linkage between two cationic subunits (Figure 3d). Reversible waves are obtained in the CVs of **Q** in the presence of **4**, indicating that the $\mathbf{4}\cdot\mathbf{Q}^{\bullet-}$ complex is stable under the experimental conditions and does not experience full proton transfer. Simulations reproduce the overall $\Delta E_{1/2}$ and the observed reversibility over the course of the titration. A mechanism involving a single binding step (K_{1Q}) with subsequent ET (E_2) is found to best describe the experimental data.[29]

As noted above, these simulations reveal that *bis*-amidinium salt **4** binds $\mathbf{Q}^{\bullet-}$as a 1:1 complex, in contrast with HBDs **1**–**3**, which form 2:1 complexes with $\mathbf{Q}^{\bullet-}$. Because of this change in stoichiometry, the efficacy of the different HBDs in promoting ET to **Q** was gauged by comparing the value of $K_{Q^{\bullet-}}$ for **4** to that of $K_{1Q^{\bullet-}}$ $K_{2Q^{\bullet-}}$ for **1**–**3**. This analysis reveals that **4** is exceptionally effective at promoting ET and is six orders of magnitude more potent than **2** at binding $\mathbf{Q}^{\bullet-}$.

Tetramethylated *bis*-amidinium salt **5**, which bears the same net charge as **4** but lacks the ability to form H-bonds, has a substantially smaller $K_{1Q^{\bullet-}}$ value than **4**. The large difference in the potency of **4** relative to **5** shows that the pronounced effect of **4** in promoting HBD-coupled ET is not purely electrostatic in nature. Instead, the combination of dual charge with hydrogen bonding capability underlies the ability of **4** to modulate the thermodynamics of ET to **Q**. Furthermore, the CVs recorded with **5** are best simulated by a pathway in which ET (E_1) precedes association ($K_{1Q^{\bullet-}}$) (Figure S5). This change in mechanism establishes that H-bonding is necessary for pre-association between **Q** and the HBD, and thereby dictates the pathway by which HBD-coupled ET occurs.

2. Kinetic Studies

Having established that dicatonic HBDs can exert a strong influence on the thermodynamics of ET to an electron-deficient quinone through tight binding of $\mathbf{Q}^{\bullet-}$, we investigated whether HBDs can similarly affect the kinetics of ET. This was addressed by measuring the rate of ET between **Q** and ferrocene (Fc) derivatives in the presence of HBDs to generate $\mathrm{HBD}\cdot\mathbf{Q}^{\bullet-}$ Fc^+ salts stoichiometrically (Table 2). Reactions were monitored using UV-vis spectrophotometry under homogeneous conditions. The rate constants were obtained under pseudo-first order conditions, with varying concentrations of excess HBD. Because the HBDs were found to span a broad range of reactivity, multiple reductants with varying reduction potentials were required for this study. Two reductants were studied with each

HBD, and the relative rates were scaled according to the intrinsic reactivity differences of those reductants.

Bis-amidinium salt **4** was found to provide remarkable acceleration of the rate of ET, with a relative rate constant that is 12 orders of magnitude larger than that for urea **3** (Table 2). A comparison of the relative rate constants with the corresponding equilibrium constants reveals a good correlation between the thermodynamics and kinetics of ET, demonstrating the ability of these HBDs to thoroughly influence the energetics of ET.

To further probe the mechanism of HBD-coupled ET and provide independent verification for the stoichiometries ascertained electrochemically, the reaction order with respect to each HBD was determined. The ET reaction obeys a second-order kinetic dependence on both guanidinium salts **1** and **2** (Figure 4a), consistent with the contention that two cationic HBDs act cooperatively to stabilize $\mathbf{Q}^{\bullet-}$. ET promoted by urea **3**, in contrast, was found to follow a first-order dependence on HBD (Figure 4b). This result may still be consistent with formation of a 2:1 complex between **3** and $\mathbf{Q}^{\bullet-}$, as a rate-determining ET step may precede complexation by the second urea molecule. The kinetic order in **4** was not accurately quantified due to the extremely high reactivity observed with this HBD. However, a Job plot obtained with excess reductant clearly shows that the reaction stoichiometry between **4** and **Q** is 1:1 (Figure S6), thereby corroborating the electrochemical thermodynamic studies.

Examining the free energy differences associated with these homogenous ETs offers a different perspective on the effectiveness of **4** as a promoter of HBD-coupled ET. ET between 1,1'-dibromoferrocene and **Q** is highly unfavorable in the absence of an HBD (ΔG_{ET} = +15.3 kcal/mol).[30] Yet **4** modulates the kinetics and thermodynamics of this inherently disfavored process such that it proceeds rapidly. In comparison, DDQ, a more powerful oxidant than **Q** that finds widespread use in organic synthesis, lacks the intrinsic reactivity to perform this ET reaction independently (ΔG_{ET} = +4.4 kcal/mol).[31] The ability of **4** to participate in HBD-coupled ET was examined further with additional electron donors, and it was found to facilitate oxidation of perylene in a yet more unfavorable process (ΔG_{ET} = +19.8 kcal/mol) [32] (Figure S7).

3. Application of HBD-coupled ET in a model synthetic transformation

With the identification of HBDs capable of promoting ET to electron-deficient quinones, we sought to probe their possible utility as catalysts for synthetic reactions involving ET. An oxidative lactonization was selected as a model transformation that would illustrate the catalytic use of HBDs to promote quinone-mediated ETs (Scheme 2a). The HBDs **1**–**4** were evaluated, and the conversions observed after 24 hour reaction times were found to correlate well with both the thermodynamic and kinetic trends discussed previously. *Bis*-amidinium salt **4** was the most effective catalyst, affording the product in 70% yield, whereas urea **3** provided no acceleration over background. The *bis*-amidinium salt **6**, which lacks the *t*-butyl substituent of **4**, proved even more reactive, affording the lactonization product in nearly quantitative yield. This difference in reactivity may be ascribed to an inductive, deactivating effect of the *t*-butyl substituent of **4**.[33]

A large KIE was measured for the lactonization (k_H/k_D=7.7 with **6**), and points to rate-limiting cleavage of the benzylic C-H bond. This can be reconciled with rapid and reversible single-electron transfer preceding a subsequent, rate-limiting H-atom abstraction (Scheme 2b), although a direct hydride abstraction mechanism cannot be ruled out unambiguously.[34] Nonetheless, the strong correlation between the effect of different HBDs on the thermodynamics and kinetics of ET to **Q** and on reaction rate in the lactonization is consistent with a mechanism in which the HBD affects a pre-equilibrium ET by binding **Q**, and remains associated with $\mathbf{Q}^{\bullet-}$ throughout the H-atom transfer.

Conclusions

As demonstrated in electrochemical and kinetic studies described above, HBD-coupled ET can be applied as an effective strategy to activate electron-deficient quinones. The application of **4** and **6** as catalysts in a model organic transformation further shows that this strategy has potential for use in synthetically useful contexts. The results obtained from this mechanistic study with simple dual hydrogen-bond donors highlight the promise of dicatonic scaffolds as catalysts for promoting ET. The evidence that association of the HBD occurs prior to ET demonstrates the potential for application of this strategy in enantioselective processes, wherein binding to the chiral catalyst prior to generation of reactive intermediates would be expected to be crucial. We expect that the findings outlined here will help guide the discovery of new catalysts capable of promoting highly efficient and selective ET reactions mediated by quinone oxidants.

Supplementary Material

Refer to Web version on PubMed Central for supplementary material.

Acknowledgments

This work was supported by the NIH (GM043214 to E.N.J.) and DOE (DE-SC0009565 to D.G.N), by an NSF pre-doctoral fellowship to A.K.T., and by an NIH post-doctoral fellowship to D.J.H. We thank Robert Knowles for many helpful discussions.

References

[1]. Taylor MS, Jacobsen EN. Angew. Chem. Int. Ed. 2006; 45:1520–1543.

[2]. Knowles RR, Jacobsen EN. Proc. Natl. Acad. Sci. USA. 2010; 107:20678–20685. [PubMed: 20956302]

[3]. Gupta N, Linschitz H. J. Am. Chem. Soc. 1997; 119:6384–6391.

[4]. Macías-Ruvalcaba NA, González I, Aguilar-Martínez M. J. Electrochem. Soc. 2004; 151:E110–E118.

[5]. Okamoto K, Ohkubo K, Kadish KM, Fukuzumi S. J. Phys. Chem. A. 2004; 108:10405–10413.

[6]. Yuasa J, Yamada S, Fukuzumi S. J. Am. Chem. Soc. 2008; 130:5808–5820. [PubMed: 18386924]

[7]. Fukuzumi S, Kitaguchi H, Suenobu T, Ogo S. Chem. Commun. 2002:1984–1985.

[8]. Gómez M, Gómez-Castro CZ, Padilla-Martínez II, Martínez-Martínez FJ, González FJ. J. Electroanal. Chem. 2004; 567:269–276.

[9]. Ge Y, Lilienthal RR, Smith DK. J. Am. Chem. Soc. 1996; 118:3976–3977.

[10]. Ge Y, Miller L, Ouimet T, K. D. J. Org. Chem. 2000; 65:8831–8838. [PubMed: 11149823]

[11]. Greaves MD, Niemz A, Rotello VM. J. Am. Chem. Soc. 1999; 121:266–267.

[12]. Clare LA, Pham AT, Magdaleno F, Acosta J, Woods JE, Cooksy AL, Smith DK. J. Am. Chem. Soc. 2013; 135:18930–18941. [PubMed: 24283378]

[13]. Mader EA, Mayer JM. Inorg. Chem. 2010; 49:3685–3687. [PubMed: 20302273]

[14]. Ferreira KN, Iverson TM, Maghlaoui K, Barber J, Iwata S. Science. 2004; 303:1831–1838. [PubMed: 14764885]

[15]. Graige MS, Paddock ML, Bruce JM, Feher G, Okamura MY. J. Am. Chem. Soc. 1996; 118:9005–9016.

[16]. Taguchi AT, O'Malley PJ, Wraight CA, Dikanov SA. J. Phys. Chem. B. 2015; 119:5805–5814. [PubMed: 25885036]

[17]. Stowell MHB, McPhilliips TM, Rees DC, Soltis SM, Abresch E, Feher G. Science. 1997; 276:812–816. [PubMed: 9115209]

[18]. Graige MS, Feher G, Okamura MY. Proc. Natl. Acad. Sci. USA. 1998; 95:11679–11684. [PubMed: 9751725]

[19]. Becker, H-D.; Turner, AB. The Chemistry of the Quinonoid Compounds Vol. II, Chapter 23. Patai, S.; Rappoport, Z., editors. Wiley; New York: 1988. p. 1352-1384.

[20]. Chambers, JQ. The Chemistry of the Quinonoid Compounds Vol. II, Chapter 12. Patai, S.; Rappoport, Z., editors. Vol. II. New York: 1988. p. 719-757.Chapter 12

[21]. Costentin C. Chem. Rev. 2008; 108:2145–2179. [PubMed: 18620365]

[22]. A large effect on the second ET is also observed with **2** and **4** (see Supporting Information for discussion).

[23]. Rudolf M. J. Electroanal. Chem. 2003; 543:23–39. DigiElch from Elchsoft under http://www.elchsoft.com.

[24]. Discrepancies in current magnitude may be attributed to variations in diffusion coefficient across the range of species involved in the simulation, which has no bearing on $\Delta E_{1/2}$ (see Supporting Information for discussion).

[25]. Efforts to simulate alternative mechanisms are described in the Supporting Information.

[26]. The pK_a values in DMSO for *N,N'*-dialkylguanidinium ions and **2** are 14.1 and 10.1, respectively. Uyeda CH. Catalysis of the Claisen Rearrangement by Hydrogen Bond Donors. 2010Ph.D. Thesis, Harvard University, Cambridge, MA

[27]. The pK_a of **3** is 13.8 in DMSO. Jakab F, Tancon C, Zhang Z, Lippert KM, Schreiner PR. Org. Lett. 2012; 14:1724–1727. [PubMed: 22435999]

[28]. Annamalai VR, Linton EC, Kozlowski MC. Org. Lett. 2009; 11:621–624. [PubMed: 19175347]

[29]. The current that appears at 0.1 V in scan (c) is not reproduced by this mechanism. This extra current has been observed in cyclic voltammograms of quinones, and has been attributed to the formation of oxides on the glassy carbon electrode surface. See: Staley PA, Newell CM, Pullman DP, Smith DK. Anal. Chem. 2014; 86:10917–10924. [PubMed: 25279716] Mechanisms involving formation of quinone dimers, which has been observed with some *o*-quinones containing electron-withdrawing groups, may also play a role in the appearance of this extra current. See: Macías-Ruvalcaba NA, Evans DH. J. Phys. Chem. C. 2010; 114:1285–1292.

[30]. Daeneke T, Mozer AJ, Uemura Y, Makuta S, Fekete M, Tachibana Y, Koumura N, Bach U, Spiccia L. J. Am. Chem. Soc. 2012; 134:16925–16928. [PubMed: 23013038]

[31]. Connelly NG, Geiger WE. Chem. Rev. 1996; 96:877–910. [PubMed: 11848774]

[32]. Cui X, Charaf-Eddin A, Wang J, Le Guennic B, Zhao J, Jacquemin D. J. Org. Chem. 2014; 79:2038–2048. [PubMed: 24517585]

[33]. A rigorous comparison of the abilities of **4** and **6** to promote ET was not possible because of the very low solubility of **6** in dichloromethane.

[34]. Guo X, Zipse H, Mayr H. J. Am. Chem. Soc. 2014; 136:13863–13873. [PubMed: 25196576]

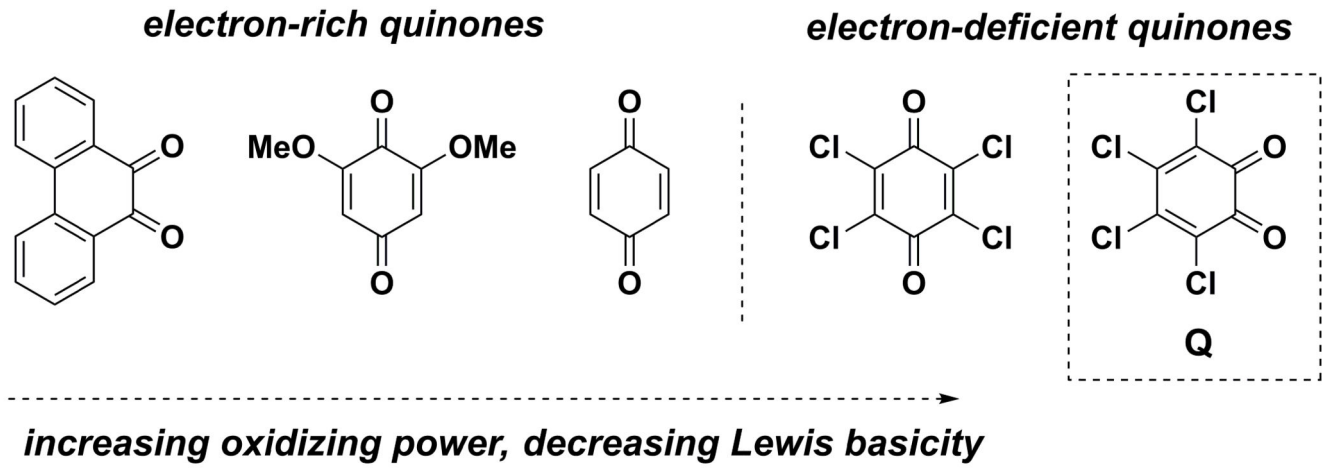

Figure 1.
Effect of quinone structure on oxidizing ability and Lewis basicity.

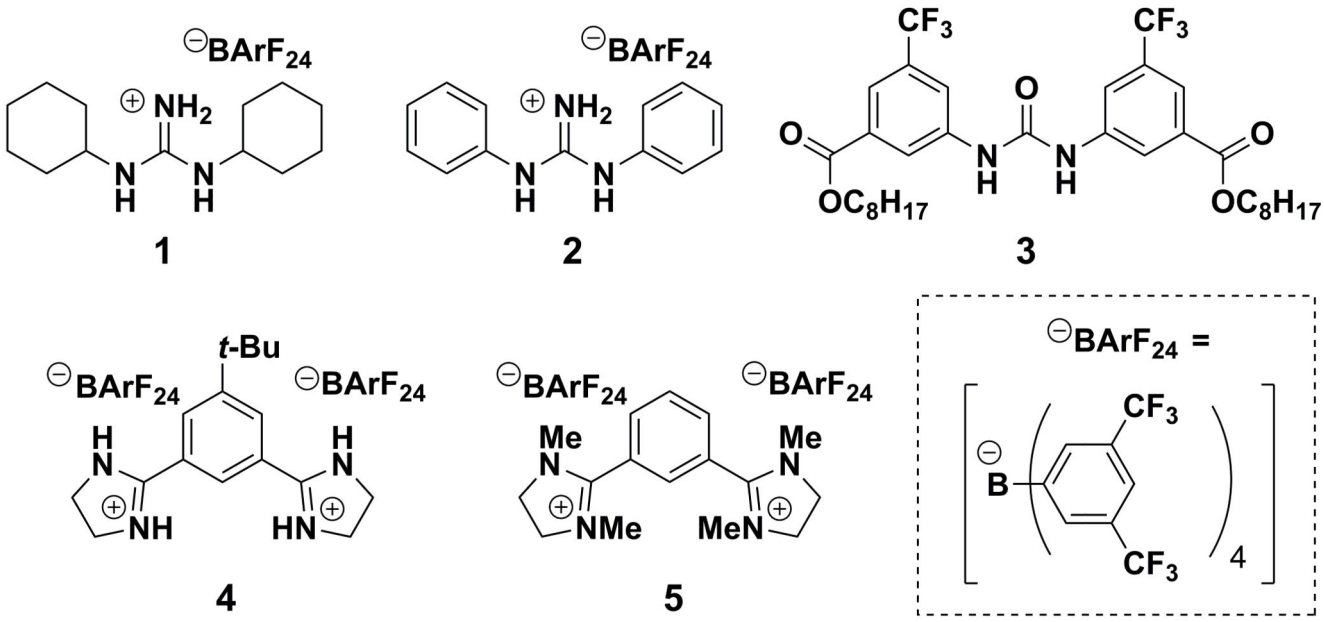

Figure 2.
Series of HBDs and additives examined in this study.

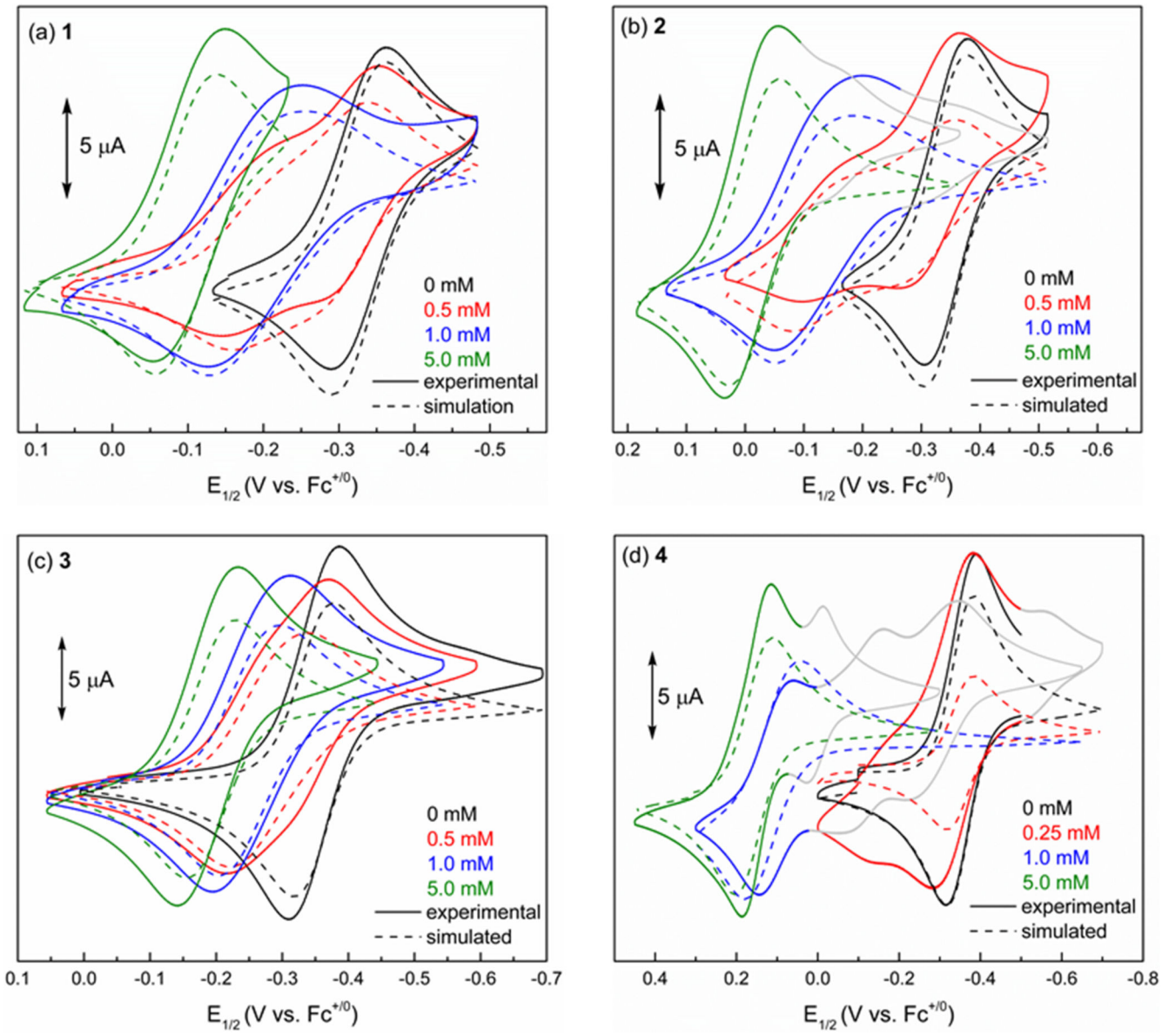

Figure 3.

Experimental CV data and comparison with simulation. CVs (0.1 V/s) recorded for 0.5 mM **Q** in 0.1 M nBu$_4$NBArF$_{24}$/CH$_2$Cl$_2$ (glovebox) in the presence of increasing (a) [**1**], (b) [**2**], (c) [**3**], (d) [**4**].

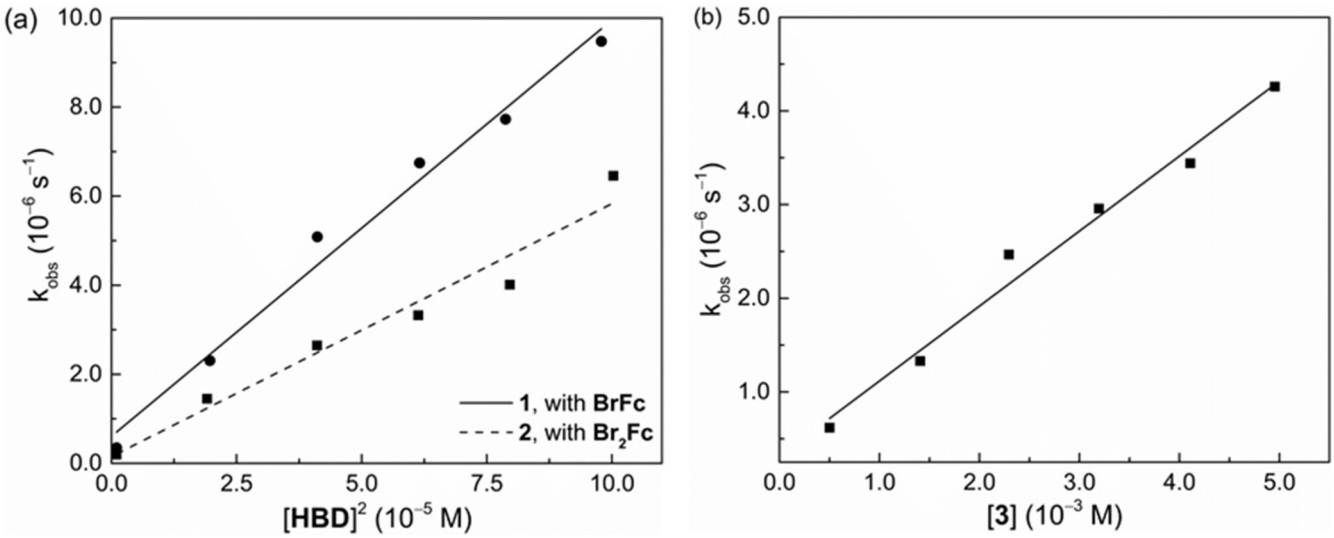

Figure 4.

Initial rate constants (k_{obs}) vs. $[HBD]^2$ or [HBD] for ET from ferrocene derivatives to **Q** in CH_2Cl_2 at 25 °C under N_2. (a) Second-order plots for **1** (10–1.0 mM), **Q** (1.0 mM), bromoferrocene (BrFc) (1.0 mM); and **2** (10–1.0 mM), **Q** (1.0 mM), 1,1'-dibromoferrocene (Br_2Fc) (1.0 mM); (b) First-order plot for **3** (5.0–0.5 mM), **Q** (0.5 mM), 1,1'-dimethylferrocene (Me_2Fc) (0.5 mM).

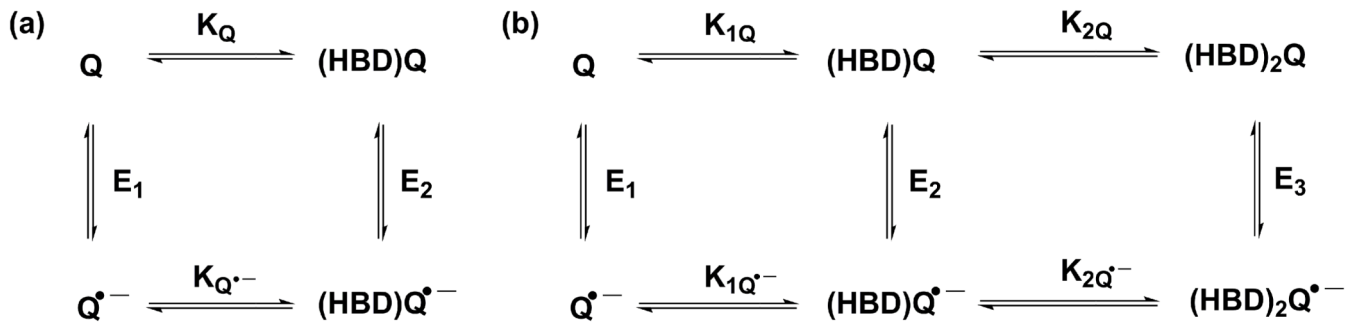

Scheme 1.

(a) Square scheme describing pathways for HBD-coupled ET to quinones and their associated equilibrium constants. (b) Extended square scheme accounting for two binding events.

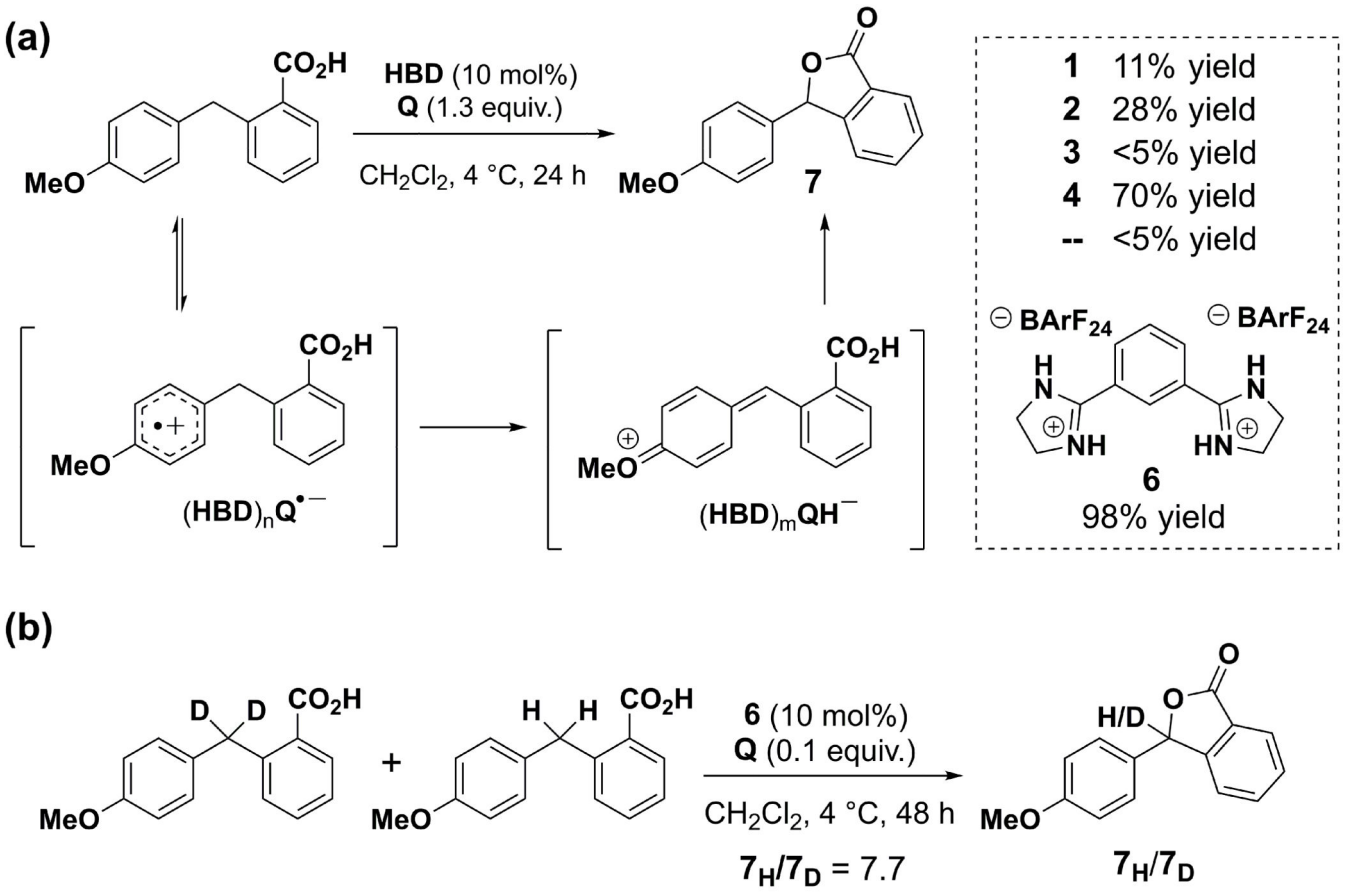

Scheme 2.

(a) Proposed oxidative lactonization mechanism and yields obtained at 24 hours. (b) Kinetic isotope effect experiment.

Table 1

Equilibrium constants for HBD-coupled ET determined by CV.[a]

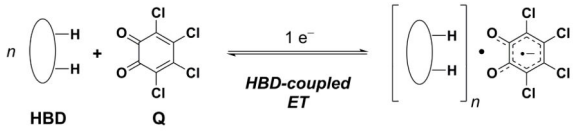

HBD[a]	$K_{1Q^{\bullet-}}$ (M^{-1})[b]	$K_{1Q^{\bullet-}}K_{2Q^{\bullet-}}$ (M^{-2})
1	(3.4×10^4)	6.1×10^8
2	(3.5×10^5)	1.8×10^{10}
3	(5.6×10^4)	1.0×10^7
4	9.2×10^{10}	--
5	5.7×10^5	--

[a] Parameters were determined by titrating 0.5 mM **Q** in 0.1 M nBu$_4$NBArF$_{24}$/CH_2Cl_2 (glovebox) with [**HBD**] and simulating the experimental CVs obtained.

[b] Values for $K_{1Q^{\bullet-}}$ in parentheses are thermodynamically redundant and are calculated from E_1, E_2, and K_{1Q}.

Table 2

Relative rate constants for HBD-coupled ET.[a]

HBD	K_{rel} (s^{-1}) Fc	k_{rel} (s^{-1}) BrFc	k_{rel} (s^{-1}) Br_2Fc	k_{rel} (s^{-1})	$K_{1Q^{\bullet-}}$ (M^{-1})	$K_{1Q^{\bullet-}} K_{2Q^{\bullet-}}$ (M^{-2})
3	1	--	--	1	5.6×10^4	1.0×10^7
1	486	1	--	4.9×10^2	3.4×10^4	6.1×10^8
2	--	124	1	2.3×10^7	3.5×10^5	1.8×10^{10}
4	--	--	104	9.0×10^{11}	9.2×10^{10}	--

[a] Pseudo-first-order rate constants were determined at 25 °C by monitoring the reaction between **Q** (2.5 mM) and the indicated ferrocene (0.5 mM) in CH_2Cl_2 in the presence of the indicated **HBD** (5.0 mM).